Octupole deformation in ^{149,151}Sm nuclei

Somapriya Basu, J. M. Chatterjee, and D. Banik
Saha Institute of Nuclear Physics, 1/AF Bidhannagar, Calcutta-700064, India

R. K. Chattopadhyay
Ananda Mohan College, 102/1 Amherst Street, Calcutta-700009, India

R. P. Sharma and S. K. Pardha Saradhi
Variable Energy Cyclotron Centre, 1/AF Bidhannagar, Calcutta-700 064, India

Parity doublet states and alternating parity bands in ^{149,151}Sm nuclei observed in ^{148,150}Nd($\alpha, 3n\gamma$) reactions at $E_\alpha = 37$ and 35 MeV are presented here. Nineteen new transitions in ^{149}Sm and sixteen in ^{151}Sm have been observed in singles and γ-γ-t-r.f. coincidence experiments. Four alternating parity bands in ^{149}Sm and two in ^{151}Sm characterized by simplex quantum numbers are reported. The observed level schemes are interpreted in terms of octupole deformation. The energy difference due to parity splitting, collective rotational parameters, quasiparticle Routhians, single particle angular momentum alignments of bands with simplex quantum number $s = \pm i$ in ^{149}Sm and with $s = -i$ in ^{151}Sm have been calculated from the experimental results. From the $E1$, $E2$ branching ratios, the electric dipole moments are deduced to be $\langle D_0 \rangle = 0.19 \pm 0.08$ e fm for ^{149}Sm and $\langle D_0 \rangle = 0.36 \pm 0.11$ e fm for ^{151}Sm. The parameter C_1, a function of the symmetry energy coefficient, has been estimated for ^{149}Sm from the liquid drop model of Strutinsky for deformed nucleus, and has been found to be $C_1 = 0.002\,003^{+0.000\,087}_{-0.000\,159}$ fm.

PACS number(s): 21.10.Ky, 23.20.Lv, 27.60.+j, 27.70.+q

I. INTRODUCTION

It is well known that the structure of transitional nuclei is very complex. The transitional character of the nuclei allows different ways of theoretical approach. The interacting boson approximation (IBA), the extended phonon projection, quasiparticle-rotor model, and various other models have been used to study the electromagnetic properties of the nuclei both in the actinide and in the lanthanide regions [1–4]. The nuclear shape determines the nature of the intrinsic states. The degeneracies and splitting of the shell-model states into less degenerate Nilsson states is considered as due to the breaking of the symmetry in transforming from spherical to prolate deformed nuclei. The symmetry breaking of Nilsson states in going to quadrupole-octupole shapes gives rise to the doubling of bands in odd-A nuclei. This feature is experimentally demonstrated in the actinide region and in the lanthanides [5–9].

In the lanthanide region, the $d_{5/2}$ and $h_{11/2}$ proton orbitals and $f_{7/2}$ and $i_{13/2}$ neutron orbitals are close to each other and to the Fermi surface, which suggests that low-lying $J^\pi = 3^-$ states should be observed in the neutron-excess rare-earth nuclei. In ^{150}Sm [5] and ^{146,148}Nd [6] interconnections between the parity doublet states through strong $E1$ transitions have been observed. Studying the differential radii of nuclei Sheline, Jain, and Jain suggested that octupole deformation may occur in the Cs ($Z = 55$) and Ba ($Z = 56$) nuclei with $N = 85$–89 [10]. The authors also predicted a sudden increase of quadrupole deformation beyond $N = 88$. A number of experiments were devoted to search for evidence of stable octupole deformation in a few rare-earth nuclei. However, experimental investigation of more nuclei is needed to verify the theoretical predictions viz. the collapse of shell gap of Nilsson orbitals, increase of quadrupole deformation at $N=88$ and Z dependence of octupole deformation near $N=90$.

We present here the experimental results of ^{149}Sm ($N = 87$) and ^{151}Sm ($N = 89$). The previous in-beam studies on the ^{149}Sm nucleus have been reported by Hammarén et al. [3], Šimecek et al. [11], and Kleinheinz et al. [12]. Hammarén et al. interpreted their results using IBA while the latter authors analyzed their observations using quasiparticle-rotor models without considering the reflection asymmetric shape of the nucleus to interpret the observed $E1$ transitions and high-spin phenomena.

Rotational bands of ^{151}Sm have been studied previously by in-beam gamma spectroscopy [13,14]. The energy levels of the observed bands were analyzed in terms of the rotation-alignment coupling scheme of the particle-plus-rotor model. Cook et al. [13] obtained different values of deformation for positive and negative parity bands and inferred the coexistence of prolate and oblate shapes. The authors with an alternate approach found that the Nilsson model with pairing and the Coriolis coupling scheme considering only β_2 deformation could not reproduce the negative parity states quite well. However, the occurrence of the parity doublet states due to reflection asymmetry and enhanced $E1$ transitions in odd-A actinide nuclei and also in ^{151}Pm motivated us to reinvestigate the odd-A Sm nuclei in the light of octupole deformation.

<u>49</u>   650

II. EXPERIMENTAL DETAILS

The experiments were performed with α beam from the variable energy cyclotron at VECC, Calcutta. The experimental procedure was standard and the preparation of the targets is described in Ref. [15]. The enriched Nd_2O_3 powder (^{148}Nd$\simeq$94%, ^{150}Nd$\simeq$96.6%) was centrifuged on kapton backings. The thicknesses of ^{148}Nd and ^{150}Nd targets varied from 4 to 10 mg/cm^2. Three HPGe gamma-x detectors—two with horizontal and one with vertical cryostat—have been used in the experiments. The relative efficiencies were 10%, 19%, and 25% for the vertical and the two horizontal detectors, respectively. The full width at half maximum (FWHM) at 1332 keV for all detectors was $\simeq$2.0 keV. The detectors shielded from background and scattered γ rays with paraffin blocks and lead bricks were placed at 90° to the beam direction and 180° and 90° relative to each other.

The cross sections of the $(\alpha, 3n)$ reactions on ^{148}Nd and ^{150}Nd, computed with the help of CASCADE-II code, peak at 34 and 33 MeV, respectively. In order to populate the higher excited states in the reactions, the projectile energies were chosen as 37 and 35 MeV for the respective targets ^{148}Nd and ^{150}Nd. Besides, with the ^{150}Nd target another set of data were recorded at $E_\alpha = 37$ MeV.

Three four-parameter γ_1-γ_2-t-r.f. coincidence experiments were performed and the events recorded on magnetic tapes for off-line analysis. r.f. gated singles data were accumulated at 35 MeV with ^{150}Nd and at 37 MeV with ^{148}Nd targets, keeping the beam current below 1 nA.

III. RESULTS

The singles spectra of ^{149}Sm and ^{151}Sm are very complex (Figs. 1 and 2). These spectra also include γ-rays belonging to the reactions other than $(\alpha, 3n\gamma)$ channels of the same targets, oxygen present in the target material, and x rays from the surrounding Pb shielding. The peaks not indicated could not be identified. Figures 3 and 4 show the coincidence spectra of ^{149}Sm and ^{151}Sm.
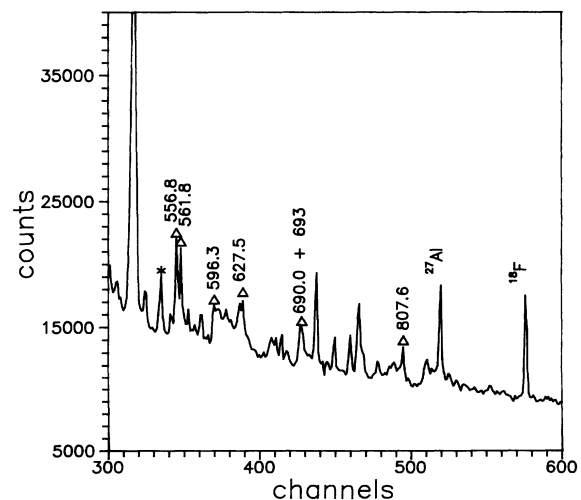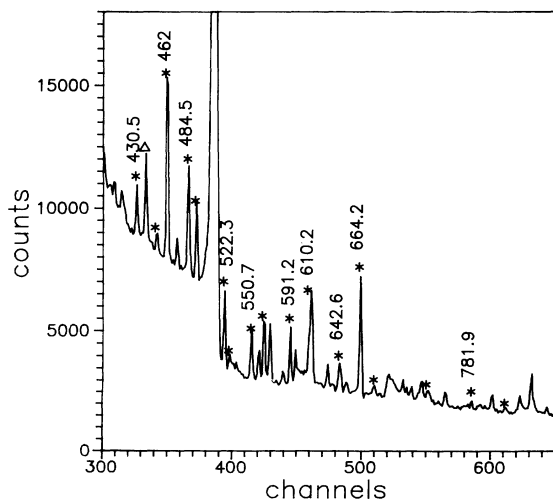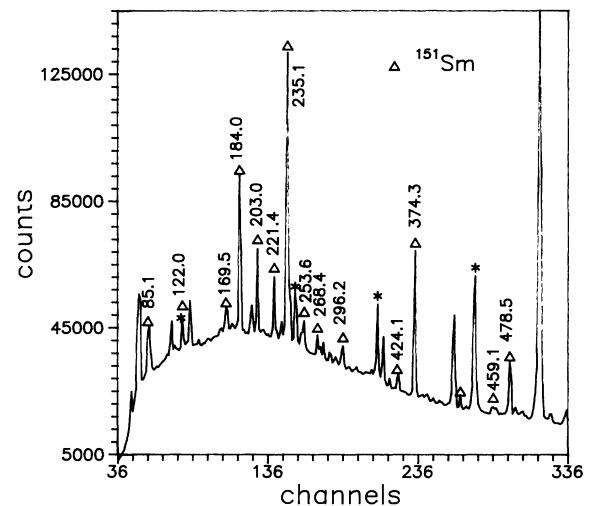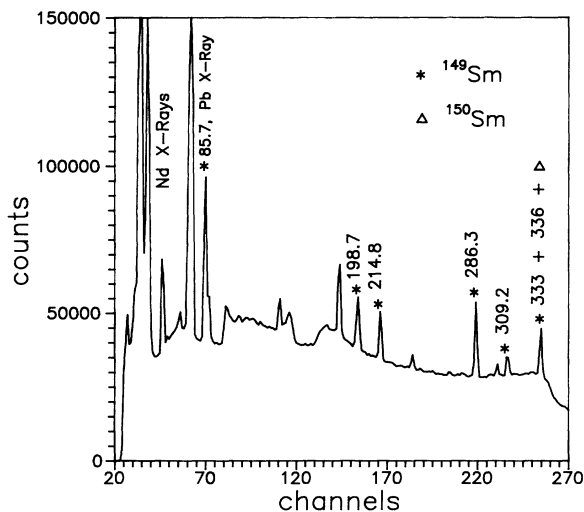
FIG. 1. Singles spectrum of ^{149}Sm from ^{148}Nd$(\alpha, 3n\gamma)$ reaction at 37 MeV. Relevant peaks are marked only. All energies in Figs. 1–6 are in keV.

FIG. 2. Relevant part of singles spectrum of ^{151}Sm at 35 MeV obtained from the ^{150}Nd$(\alpha, 3n\gamma)$ reaction. The asterisk indicates γ peaks of reactions other than $(\alpha, 3n\gamma)$.

A. ^{149}Sm nucleus

In Table I, energies of γ rays observed in this experiment and their relative intensities are given. Nineteen new transitions along with those reported in Ref. [3] have been observed in the present work. The transitions observed in the γ-γ coincidence studies are given in Table II. In Fig. 3, 462 and 664 keV gated spectra are shown.

A partial level scheme of ^{149}Sm (Fig. 5) displays the interband and the intraband transitions, the thickness of the arrows indicate the intensities. The γ lines previously unknown have been placed in the decay scheme from intensity and energy difference considerations and their presence in the multiple gated spectra. The spins and parities of the levels shown in the scheme have been taken from the Refs. [3,11,16]. The values within parentheses have been assigned tentatively from the ratios of the transition probabilities $T(E1)/T(E2)$ of the new levels, observation of cascade γ rays in different gated spectra, and intensity balance of the γ transitions.

The two negative parity bands built on $f_{7/2}[514]$ and $h_{9/2}[505]$; two positive parity bands on $i_{13/2}[633]$ and [624] are shown in the level scheme (Fig. 5). A new band built on the 1193 keV level ($J^\pi = \frac{13}{2}^-$) has also been included. Both the positive parity bands originating from the $i_{13/2}$ orbital follow the $\Delta I = 2$ excitations. The band built on the 879 keV level is connected with the $f_{7/2}[514]$ ground-state rotational band ($\Omega = \frac{7}{2}^-$) whereas the band on the 789 keV level ($\Omega = \frac{7}{2}^+$) is interconnected with the negative parity band originating from $h_{9/2}[505]$ state by strong $E1$ transitions. A side band built on 1309 keV level ($J^\pi = \frac{11}{2}^-$) [3,12] has also been observed but not included in the level scheme.

B. ^{151}Sm nucleus

The singles spectrum of ^{151}Sm contains a few impurity peaks similar to those in ^{149}Sm. Sixteen new γ rays in addition to the previously reported transitions [13,14,22]

FIG. 3. Partial coincidence spectra of interest of ^{149}Sm nucleus gated with (a) 462 keV (b) 664 keV γ rays; the asterisk indicates γ peaks belonging to this nucleus.
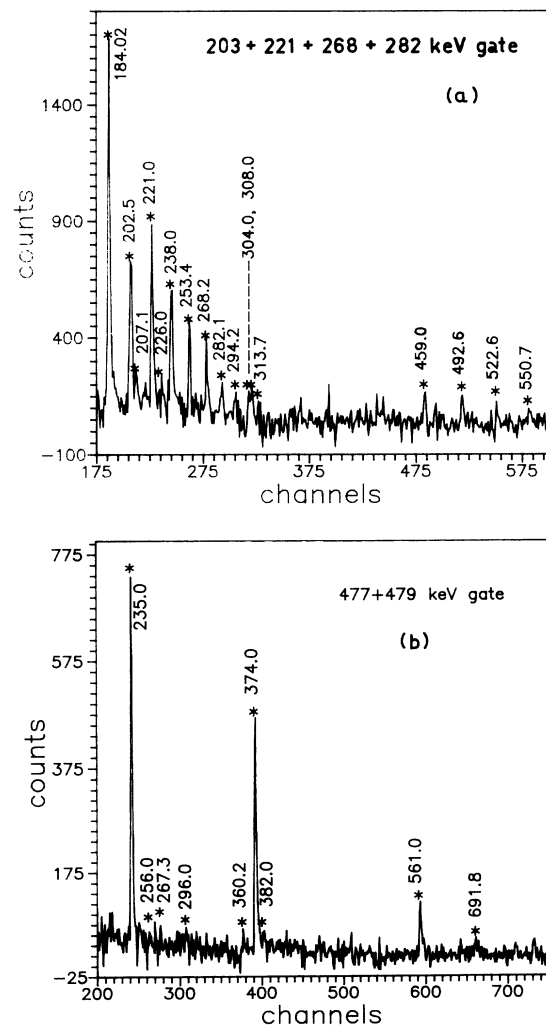
FIG. 4. (a) Added coincidence specturm of ^{151}Sm gated with 203+221+268+282 keV and (b) 477+479 keV γ-rays; γ peaks belonging to ^{151}Sm nucleus are marked by the asterisk.
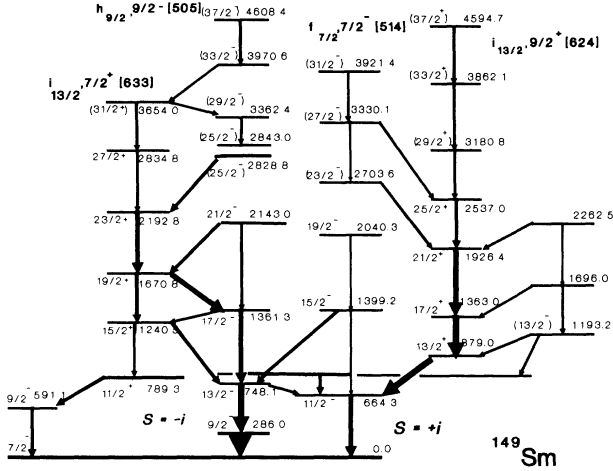
FIG. 5. Relevant level scheme of ^{149}Sm.

considered in evaluating the relative intensities of γ transitions of ^{151}Sm. Figure 4 shows the 203+221+268+282 and 477+479 keV gated spectra. The peaks observed in the different gates are tabulated in Table IV.

A strongly populated positive parity band built on the 91.5 keV level ($J^{\pi} = \frac{9}{2}^{+}$) and a negative parity band on $h_{11/2}$ state ($J^{\pi} = \frac{11}{2}^{-}$) are shown in the partial decay scheme of ^{151}Sm (Fig. 6). The negative parity band has been extended to a level of energy 3133 keV and is interconnected with the band on $\frac{11}{2}^{+}$ [615] through $E1$ transitions. Unlike ^{149}Sm, strong $M1$ transitions are observed in the negative parity band. Above the excitation energy of 2205 keV, regularity of this band disappears, which is possibly due to the interplay between the single particle and collective mode of excitations [15].

The positions of the weakly populated states $\frac{11}{2}^{+}$, $\frac{15}{2}^{+}$, $\frac{19}{2}^{+}$, $\frac{23}{2}^{+}$, ..., sequence in the $N = 6$ positive parity band was previously predicted [13]. We have extended this band to an excitation energy of 2686 keV. If this band is the missing member of $\frac{9}{2}^{+}$, $\frac{13}{2}^{+}$, ... sequence of levels we should also observe the $\frac{11}{2}^{+}$ state. In our coincidence experiment we observe two γ rays 256.4 and 267.7 keV which may decay sequentially from the 672 keV level ($J^{\pi} = \frac{15}{2}^{+}$) through 415.6 keV level (previously unknown) to 147.9 keV level ($J^{\pi} = \frac{13}{2}^{+}$). We assign this new level and the transitions tentatively and they are shown by broken lines in Fig. 6.

have been observed. Table III gives E_{γ} (keV) with intensity I_{γ} relative to the intensity (100%) of the 374 keV γ ray used instead of the strongest 235 keV transition. The coincident spectra gated with two intense γ rays 122 and 245 keV belonging to ^{152}Sm show the presence of a weak 235 keV line and hence this γ ray has not been

TABLE I. The relative intensities of γ rays observed in ^{149}Sm.

E (keV)	Relative intensity	E (keV)	Relative intensity
84[a]		527.1[b]	>5.44
121±0.8	4.55±0.12	532±1.6	5.37±0.27
125±0.8	3.01±0.11	563.4±1.6	24.48±0.41
198.2±0.9	39.53±0.31	566[b]	1.36±0.31
214.7±0.95	48.64±0.34	591.1±1.7	20.53±0.41
266.86±1.1	2.03±0.11	610.6±1.7	19.00±0.9
272.02±1.1	3.02±0.17	613.3±1.7	39.79±0.54
283.68±1.1	4.30±0.17	626±1.7	2.04±0.20
286.0±1.10	100.0	635.3±1.7	2.57±0.18
292[b]	<0.21	637[a]	
296.37±1.2	2.61±0.26	642.0±1.7	9.71±0.33
309.4±1.20	37.25±0.41	644±1.7	7.08±0.30
314.2+316.7±1.20	1.29±0.11	649.9±1.7	4.93±0.23
333.5+336[b]	<7.31	664.3±1.7	51.66±0.64
403.5±1.4	1.69±0.12	681.8±1.7	2.46±0.26
430.3±1.5	13.27±0.40	732.6±1.8	3.13±0.23
451.3±1.5	7.62±0.33	736.0±1.8	3.01±0.24
462.0±1.5	65.27±0.60	776[a]	
472.5±1.5	12.34±0.34	781.6±1.8	2.95±0.24
492.8±1.5	25.17±0.43	791.8±1.8	0.95±0.13
502.4±1.6	14.01±0.32	818.0±1.8	0.72±0.06
519[b]	<0.14	1023.2±1.9	3.67±0.37
522.0±1.6	23.58±0.40		

[a]Observed in different gated spectra.
[b]Intensity limit set from coincidence spectra.

IV. DISCUSSIONS

A. Simplex quantum number

The common feature of even-even and odd-A nuclei in the mass region $A \sim 150$ is the appearance of low-lying positive and negative parity bands. This being the transitional region, pure rotational bands cannot be expected and coexistence of symmetric and asymmetric shapes are predicted [17,18]. However, the two odd-A Sm nuclei studied here differ significantly. While in ^{149}Sm parity doublet states and two sets of alternating parity bands

have been observed—interconnected by strong $E1$ transitions, in ^{151}Sm such interconnections between only one set of alternating parity bands is primarily confined to the lower excitation region through $E1$ modes.

In the reflection asymmetric nuclear field, the intrinsic Hamiltonian H_{intr} does not commute with the parity operator P but is invariant under the combined symmetry RP (R rotates the nucleus through an angle π about an axis perpendicular to the symmetry axis) when the nuclear deformation has the odd multipole components. Under these circumstances, neither P nor R has eigenstates in the intrinsic frame. The symmetry operator is

TABLE II. The γ transitions observed in various gates of ^{149}Sm.

Gates (keV)	γ transitions observed, in keV
198	121, 309, 316, 403, 430, 451, 503, 522, 566, 591, 636, 638, 642
214	314, 336, 484, 503, 532, 563, 566, 610, 644, 681, 738
286	121, 125, 309, 430, 462, 484, 492, 519, 522, 527, 613, 637, 642, 650, 818, 1022
309	121, 198, 286, 462, 472, 522, 613, 642, 818
430	198, 286, 462, 492, 522, 635, 642, 818
462	286, 309, 316, 430, 472, 492, 519, 522, 608, 613, 637, 642, 650, 665, 781, 788
333+336	214, 462, 484, 563, 664
403	125, 198, 286, 462, 503, 566
472	232, 286, 309, 430, 451, 462, 492, 613
484	90, 198, 214, 286, 333, 336, 563, 591, 610, 644, 664, 739, 776
492	121, 286, 309, 316, 430, 462, 522, 600, 608, 642, 782, 818
522	85, 121, 125, 198, 286, 292, 309, 317, 379, 430, 451, 462, 492, 527, 613, 642, 818
563	198, 214, 286, 484, 591, 610, 664, 792
591	90, 121, 198, 214, 314, 430, 472, 484, 492, 503, 563, 635, 642
610+613	85, 99, 198, 214, 286, 309, 314, 462, 484, 522, 563, 570, 640, 644, 664, 681, 732, 792
642+644	214, 286, 309, 317, 522, 527, 563, 591, 610, 613, 664
664	85, 90, 125, 214, 266, 272, 286, 314, 333, 336, 403, 451, 462, 484, 503, 522, 563, 591, 610, 613, 626, 644, 661, 681, 733, 736, 776, 792
790	198, 214, 286, 563, 626, 664

connected with P and R by

$$S = PR^{-1} . \qquad (1)$$

The eigenvalue s of the S operator is called the simplex quantum number, which is used to classify these parity doublet states [19,20].

In ^{149}Sm, $s = i$ can be assigned to the sequence $\frac{7}{2}^-$, $\frac{11}{2}^-$, $\frac{13}{2}^+$, $\frac{15}{2}^-$, ..., ($\frac{9}{2}^+$ being unobserved) and $s = -i$ to the sequence $\frac{9}{2}^-$, $\frac{11}{2}^+$, $\frac{13}{2}^-$, $\frac{15}{2}^+$, $\frac{17}{2}^-$, ..., ($\frac{7}{2}^+$ being unobserved). On the other hand, only one $s = -i$ band with states $\frac{11}{2}^+$, $\frac{13}{2}^-$, $\frac{15}{2}^+$, ... has been identified in ^{151}Sm in these measurements.

B. Parity splitting and energy splitting

In a sequence of alternating parity states energy splitting and displacement of levels with opposite parity occurs due to the finite barrier tunnelling between the left- and right-hand orientation of the system. The energy difference of the split levels δE can be evaluated from the experimental results using the relations

$$\delta E = E(I^+) - \frac{(I+1)E(I-1)^- + IE(I+1)^-}{2I+1} . \quad (2)$$

The second term is an interpolated level of same spin but opposite parity, obtained by means of the $I(I + 1)$ rule from the two adjacent negative parity states of the same simplex band. Figures 7(a) and 7(b) compare δE vs $(I - I_0)$ curves of ^{148,149}Sm and ^{150,151}Sm, I_0 being the ground-state spin. The striking similarities of the nature of δE for odd-A Sm nuclei with even-even Sm are indications of the occurrence of a similar type of shape change. The difference in values of energy difference δE as a function of $(I-I_0)$ for $s = \pm i$ bands is interpreted as due to the combined effect of both parity and signature splitting [19]. In the limit of stable octupole deformation, δE should be close to zero and, at the same limit, the ratio between the rotational frequencies of the positive and negative parity bands,

$$\frac{\omega^+(I)}{\omega^-(I)} = 2\frac{E(I+1)^+ - E(I-1)^+}{E(I+2)^- - E(I-2)^-} , \qquad (3)$$

should approach unity. Figure 8 shows the variation of the ratio ω^+/ω^- with $(I - I_0)$ for the nuclei under study. In case of ^{149}Sm, both δE and ω^+/ω^- show their respec-

TABLE III. The relative intensities of γ rays observed in ^{151}Sm.

E (keV)	Relative intensity	E (keV)	Relative intensity
56.6±0.7	0.23±0.02	356.0±1.3	15.16±0.87
65.9±0.7	5.48±0.06	360.5±1.3	1.18±0.086
85.1±0.7	8.97±0.06	374.3±1.4	100.00
109.7±0.7	6.83±0.07	382.3±1.4	4.62±0.51
113.4±0.8	1.23±0.06	387.0±1.4	6.78±0.61
169.5+169.7±0.8	9.80±0.98	424.9[a]±1.5	11.64±0.49
175.4+176.9±0.8	2.08±0.08	459.1±1.5	7.59±0.59
184.02+185.1±0.9	10.46±0.10	462.0±1.5	5.65±0.52
195.2+197.1±0.9	3.81±0.30	476.4±1.5	7.24±0.46
203.0±0.9	27.45±0.51	478.5±1.5	53.10±0.92
207.4±0.9	1.70±0.51	488.9±1.5	4.27±0.14
221.0±1.0	20.56±0.48	491.9±1.5	8.34±1.38
226.8±1.0	1.04±0.06	496.0±1.5	3.33±1.40
235.1±1.0	128.42±0.72	504[b]	<3.99
238.0±1.0	24.26±0.80	522.1±1.6	6.07±1.46
253.6±1.0	10.50±0.36	550.8±1.6	6.94±0.64
256.0[c]		556.5±1.6	27.14±2.36
266.0±1.1	1.21±0.06	561.4±1.6	25.47±1.33
268.4±1.1	8.12±0.41	575.9±1.7	2.10±0.73
282.2±1.1	7.90±0.76	596.4+597.7±1.7	25.47±0.33
288.5±1.2	8.68±0.97	614.0±1.7	1.68±0.13
294.0±1.2	7.94±0.13	626.9±1.7	8.56±3.02
296.2±1.2	13.32±0.81	671.0±1.7	10.52±0.85
303.5±1.2	1.87±0.78	691.0±1.7	10.52±0.84
308.1±1.2	1.84 ±0.06	745.1±1.8	13.74±2.32
311.4±1.2	2.67±1.67	774.3±1.8	3.49±1.33
313.9[b]	<4.10	808.6±1.8	6.38±0.35
346.9±1.3	5.57±0.46		

[a]Doubly placed.
[b]Intensity limit set from coincidence spectra.
[c]Observed in different gated spectra.

SOMAPRIYA BASU *et al.*

TABLE IV. The γ transitions observed in various gates of ^{151}Sm.

Gates (keV)	γ transitions observed (keV)
175	85, 357, 462, 497
184	56, 66, 86, 109, 114, 175, 185, 203, 207, 221, 226, 238, 254, 268, 283, 294, 304, 308, 311, 314, 383, 424, 460, 492, 522, 551, 575, 598, 694, 808
203	56, 66, 86, 109, 114, 122, 170, 175, 184, 221, 238, 254, 268, 283, 294, 304, 308, 311, 314, 460, 522, 551, 575, 596, 808
207	114, 184, 203, 221, 238, 254, 283, 288, 294, 304, 596, 808
221	56, 66, 86, 109, 170, 175, 184+185, 203, 207, 238, 254, 268, 283, 294, 304, 311, 387, 476, 492, 505, 522, 556, 575, 596+598, 808
226	184, 283, 304, 476
235	92, 288, 296, 374, 383, 476, 478, 489, 561, 598, 626, 671, 691, 760, 775
238	122, 175, 184, 203, 207, 221, 226, 254, 268, 283, 288,[a] 304, 308, 314, 374,[a] 383, 424, 460, 478,[a] 522, 575, 596, 614
251+254	66, 122, 184, 203, 221, 238, 268, 294, 387, 424, 460, 505, 551, 556, 596
268	56, 66, 86, 114, 169, 184, 195, 203, 207, 221, 254, 283, 288, 296, 304, 308, 311, 347, 356, 383, 424, 460, 492, 505, 575, 694, 808
283	56, 86, 114, 122, 170, 184, 195, 207, 221, 268, 294, 347, 387, 424, 460, 522, 598, 694
294+296	122, 184, 203, 221, 235, 254, 268, 283, 304, 308, 311, 374, 387, 424, 478, 492, 551, 556, 598, 808
303	184, 221, 238, 268, 283, 294, 311, 424
308	56, 170, 184, 203, 207, 221, 235, 288, 294, 424
311	56, 203, 221, 238, 254, 283, 294, 311, 424
374	92, 235, 296, 478, 489, 556, 561, 598, 691, 745, 775
383	170, 207, 235, 288, 308, 476, 556, 598
424	66, 114, 122, 170, 175, 184+185, 195, 235, 238, 254, 268, 294, 314, 374, 492, 522, 551, 575, 614, 671, 745, 775
477+479	185, 235, 256, 268, 296, 360, 561, 598, 671, 691, 745, 775
489	235, 374, 478
492	56, 92, 170, 175, 184, 195, 203, 221, 268
496	175, 357, 462
556	114, 175, 235, 288, 374, 383, 476, 478, 598, 671
561	235, 374, 478, 489, 626
598	122, 170, 185, 226, 235, 374, 383, 478, 775

[a]Observed due to the presence of 235 keV in the 238 keV gate.
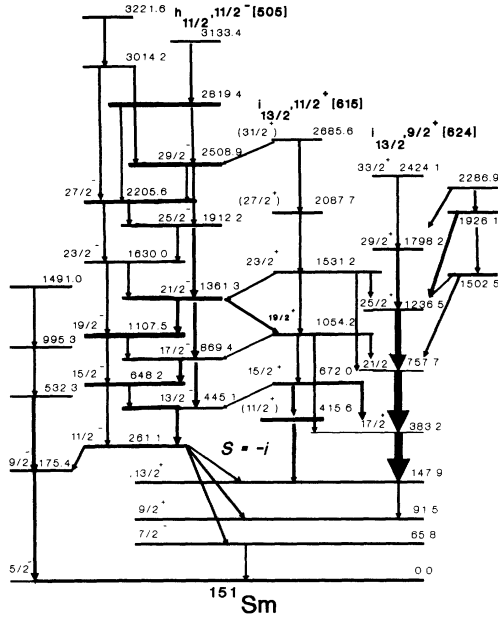
FIG. 6. Patial level scheme of ^{151}Sm showing the band denoted by $s = -i$.

tive characteristics for stability at $(I - I_0) \sim 9\hbar$. Around this spin this nucleus with octupole correlations probably develops an octupole shape. Similar behavior is seen in ^{151}Sm at $(I - I_0) \sim 10\hbar$.

C. Rotational properties of ^{149}Sm and ^{151}Sm

The parity doublet states in ^{149}Sm are identified with $\frac{7}{2}^+[633]$, $\frac{7}{2}^-[514]$, and $\frac{9}{2}^+[624]$, $\frac{9}{2}^-[505]$ Nilsson orbitals. However, the states of the opposite parity members of these doublets form two rotational bands if states connected by $E1$ and $E2$ transitions are grouped together. These rotational bands are denoted by $s = \pm i$ and have $K = \frac{7}{2}$ (Fig. 5). But in ^{151}Sm, although parity doublet states are present, one rotational band with $K = \frac{11}{2}$ is formed on $\frac{11}{2}^+[615]$ and $\frac{11}{2}^-[505]$. In the present work the $E1$ transitions between the $s = -i$ bands for both the nuclei are found to be favored.

The rotational frequency ω, the aligned angular momentum along the rotational axis I_x, and the effective moment of inertia I_{eff} have been calculated from the energies of the observed states with constant parity p and simplex s using the formulas

$$\omega(I) = \frac{E(I+1) - E(I-1)}{I_x(I+1) - I_x(I-1)} , \tag{4}$$

$$I_x(I) = [(I + \tfrac{1}{2})^2 - K^2]^{1/2} , \tag{5}$$

$$I_{\text{eff}} = I_x(I)/\omega(I) . \tag{6}$$

The I_x vs rotational frequency ω plot is displayed in Fig.
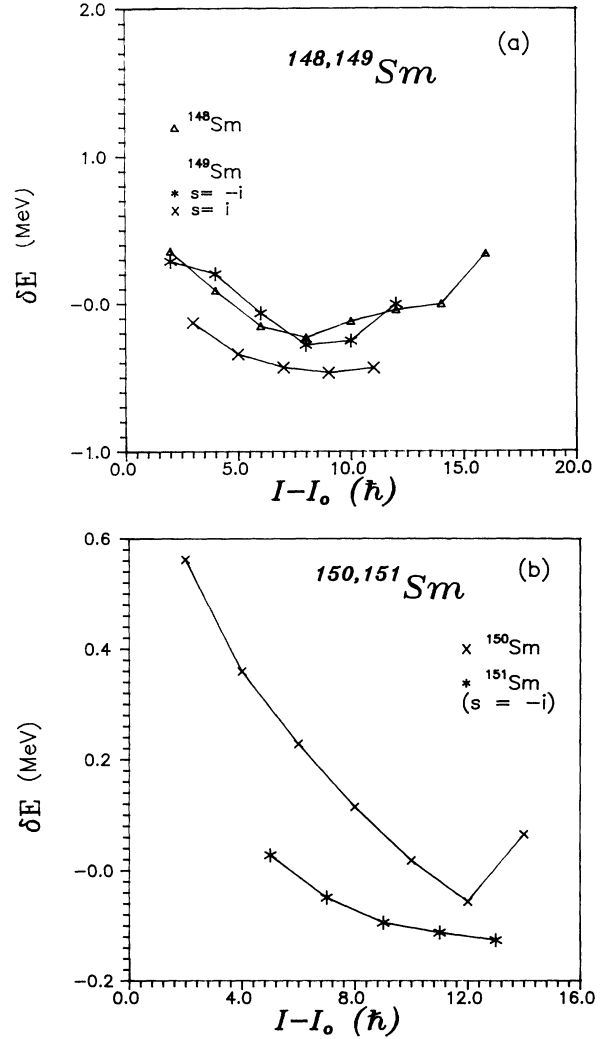
FIG. 7. (a) δE deduced from the level energies of ^{149}Sm and compared with the results of ^{148}Sm, level energies of ^{148}Sm have been taken from Ref. [30]; (b) similar results but of ^{151}Sm compared to those of ^{150}Sm, energy values of ^{150}Sm taken from Ref. [5].
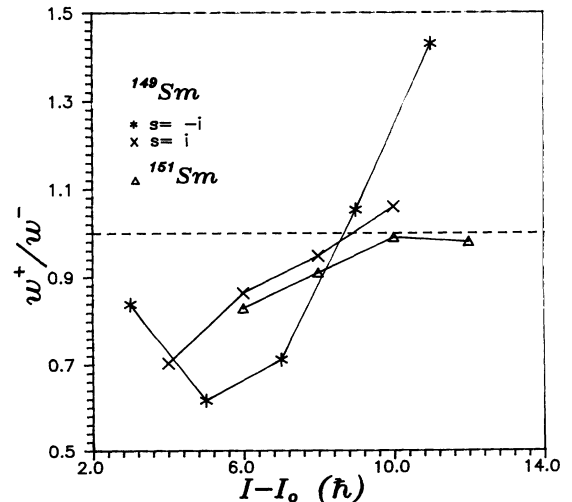
FIG. 8. Variation of ω^+/ω^- as a function of $(I - I_0)$ for ^{149,151}Sm.

9, while that of the I_{eff} as a function of ω is shown in Fig. 10.

A common property of these two nuclei is that the moment of inertia of the opposite parity band is larger than that of ground-state band, irrespective of simple quantum number, and approaches a common value with rotation. This in the case of ^{222}Ra was explained by Bonche *et al.* by performing a self-consistent Hartree-Fock calculation taking into account the octupole degrees of freedom [21]. They observed that the quadrupole deformation is larger for the opposite parity band than that of ground-state band and hence a larger value of the moment of inertia. This specific characteristic was also reported in octupole deformed ^{221,223}Th [19].

In ^{149}Sm nucleus, a sharp backbending or upbending of I_{eff} and I_x is observed around $\hbar\omega \simeq 0.3$ MeV. A similar feature has been reported in ^{150}Sm [5] and also in ^{219}Ra [20] and ^{221,223}Th [19] but at a lower frequency. This phenomenon has been interpreted as due to the sudden increase of octupole strength with rotation, caused by weaker pairing correlations and also by enhanced oc-

tupole mixing between the single-particle states of opposite parity [29].

The experimental Routhians E' can be calculated from

$$E'(I) = \tfrac{1}{2}[E(I+1) - E(I-1)] - \omega I_x(I) \qquad (7)$$

and are shown in Figs. 11(a) and 11(b) for ^{149}Sm and ^{151}Sm, respectively. The quasiparticle Routhians can be evaluated from the expression (7) by subtracting a reference configuration. For the odd nucleus, the reference values are obtained by averaging over the two even-even neighbors, taking into consideration the odd-even mass difference Δ. The experimental quasiparticle Routhians can be computed by using

$$\begin{aligned} e'(A, \omega) &= E'(A, \omega) + \Delta \\ &\quad - \tfrac{1}{2}[E'_g(A+1, \omega) + E'_g(A-1, \omega)] \,. \end{aligned} \qquad (8)$$

Similarly the single-particle aligned angular momentum has been estimated from
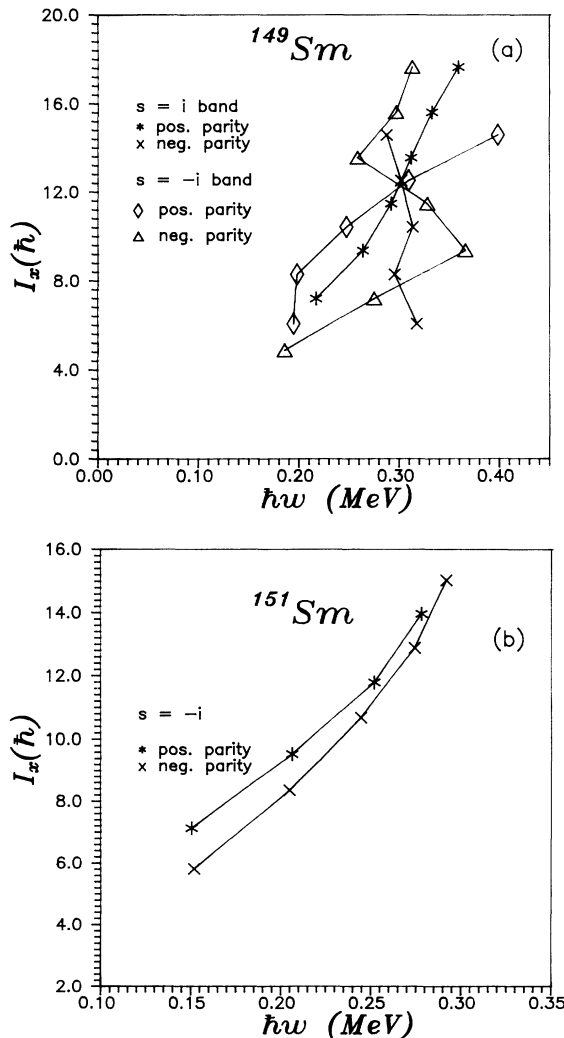
FIG. 9. Aligned angular momentum I_x as a function of rotational frequency ω for (a) ^{149}Sm; (b) ^{151}Sm.
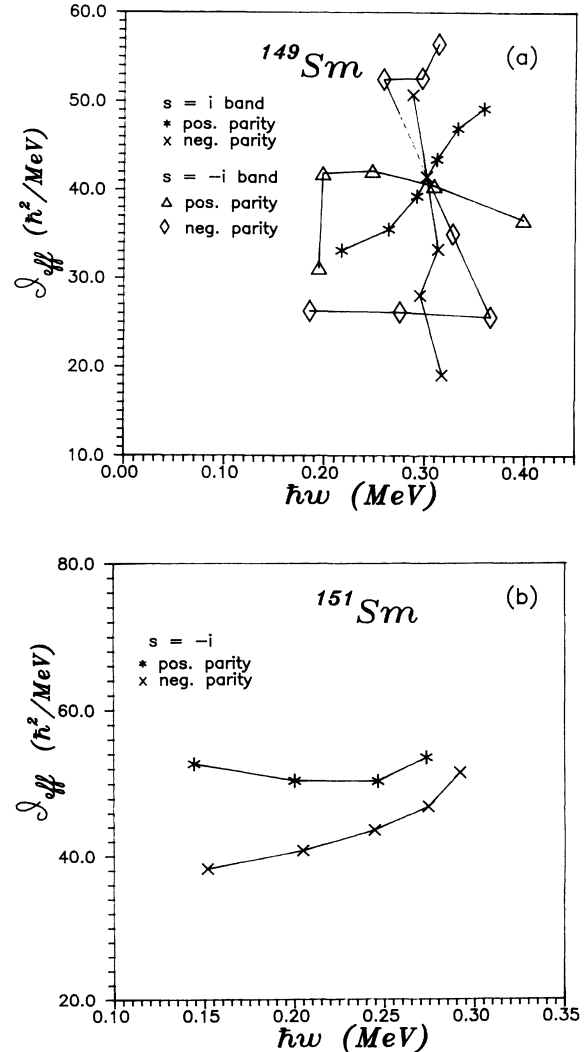
FIG. 10. Effective moment of inertia I_{eff} vs rotational frequency ω (a) for positive and negative parity bands with $s = \pm i$ for ^{149}Sm; (b) similar results with $s = -i$ for ^{151}Sm.

$$i'(A,\omega) = I_x(A,\omega) - \tfrac{1}{2}[I_x^g(A+1,\omega) + I_x^g(A-1,\omega)] ,$$

(9)

where I_x^g refer to the aligned angular momentum for the ground-state band of the even-even neighbors. These curves are displayed in Figs. 12 and 13 for ^{149}Sm and ^{151}Sm. In the ^{149}Sm nucleus, it is observed that the $e'(A,\omega)_{\text{exp}}$ for positive parity bands with $s = \pm i$ come closer at $\hbar\omega \simeq 0.3$ MeV, the frequency with spin $I \simeq 9\hbar$, where $\delta E \simeq 0$ and $(\omega^+/\omega^-) \simeq 1$. The most interesting result is the alignment of the single-particle angular momentum, which increases with rotational frequency and attains a maximum value. Above $\hbar\omega \simeq 0.3$ MeV, this alignment is quenched. The divergence of the I_{eff} and $I_x(I)$ above $I \simeq 9\hbar$ ($\hbar\omega \simeq 0.3$ MeV) is possibly due to this quenching of angular momentum alignment. The nucleus above this frequency seems to change its shape [29].

The ^{151}Sm nucleus with two neutrons more than ^{149}Sm exhibits a different behavior. The $i'(A,\omega)$ curves for the

positive parity bands are almost constant up to $\hbar\omega \simeq 0.28$ MeV, beyond which it seems to increase. The experimental quasiparticle Routhians $e'(A,\omega)$ for these bands have negative slope, meet at $\hbar\omega \simeq 0.25$ MeV, and follow the same path thereafter as in Fig. 13(b), indicating that both these bands originate from the same intrinsic structure.

D. Electric dipole moment

The nucleus which has an octupole deformation in addition to the quadrupole deformation, mainly decays through $E1$ and $E2$ transitions. The intrinsic dipole moment D_0 and intrinsic quadrupole moment Q_0 can be deduced using the following formulas from the particle-plus-rotor model,

$$\left(\frac{D_0}{Q_0}\right)^2 = \frac{5}{8}\frac{B(E1)}{B(E2)}\frac{(I+K-1)(I-K-1)}{(2I-1)(I-1)} .$$

(10)

We found the $B(E1)/B(E2)$ values by using the expres-
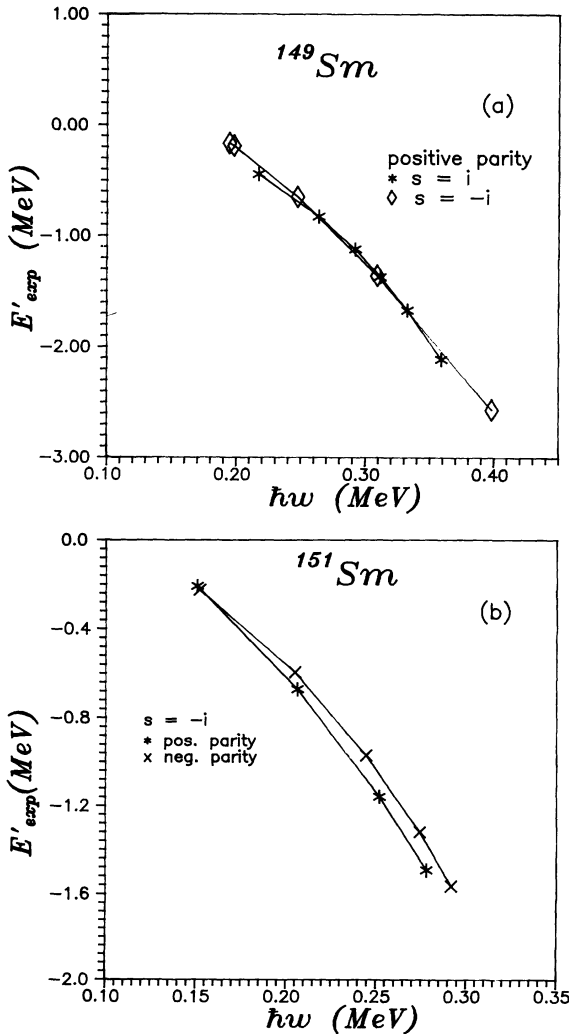
FIG. 11. Experimental Routhians as a function of ω, (a) for positive parity bands of ^{149}Sm with $s \pm i$; (b) for positive and negative parity bands of ^{151}Sm with $s = -i$.
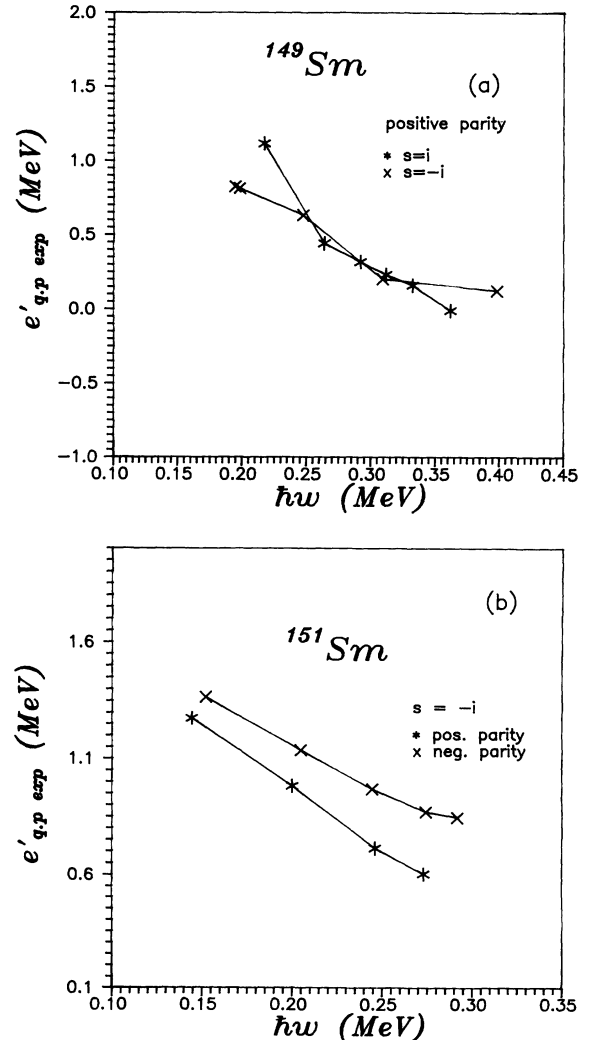
FIG. 12. Quasiparticle Routhians derived from the results of Fig. 11; (a) ^{149}Sm, (b) ^{151}Sm.
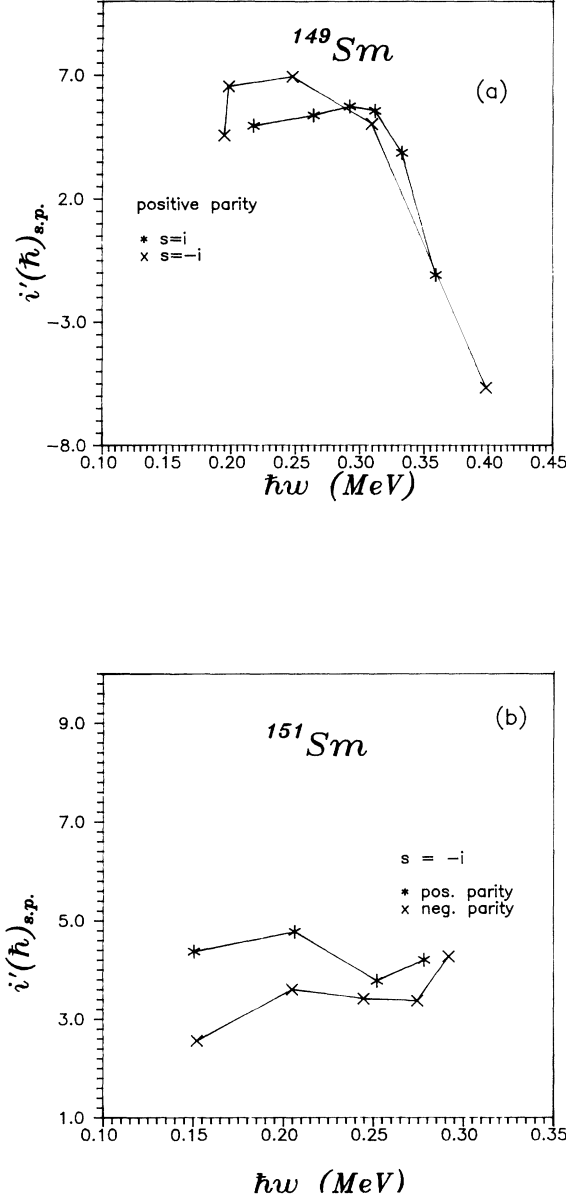
FIG. 13. Aligned single-particle angular momenta estimated from the results of Fig. 9; (a) of ^{149}Sm, (b) of ^{151}Sm.

sion

$$\frac{B(E1)}{B(E2)} = \frac{I_\gamma(E1)}{I_\gamma(E2)} \frac{E_{\gamma(2)}^5}{E_{\gamma(1)}^3} 7.1 A^{2/3} (10^{-7} \text{ fm}^{-2}) \qquad (11)$$

of Ref. [9], where the intensities and energies have been taken from the present work.

The values of Q_0 can be estimated from the experimental ground-state quadrupole moments Q [23,24] using the expression (Ref. [25])

$$Q_0 = \frac{(I+1)(2I+3)}{3K^2 - I(I+1)} Q . \qquad (12)$$

The dipole moment D_0 has then been calculated by means of Eq. (10) for each level. For both ^{149}Sm and ^{151}Sm, $B(E1)/B(E2)$, Q_0, and D_0 values are almost independent of spin within the limits of error (Table V), and also depend neither on parity nor on simplex quantum number. The average values of $\langle D_0 \rangle$ is 0.19 ± 0.08 e fm for ^{149}Sm and for ^{151}Sm it is 0.36 ± 0.11 e fm. Column 5 of Table V contains the $B(E1)/B(E2)$ ratios for ^{149,151}Sm which are comparable to those of ^{148}Sm [17]. D_0 determined from these branching ratios have been close to the theoretically calculated electric dipole moment $D_0 = 0.2$ e fm with octupole deformation $\beta_3 = 0.05$ for ^{148}Sm [17]. In the case of ^{151}Sm, the higher value of $\langle D_0 \rangle$ is due to a higher experimental ground-state quadrupole moment Q.

The dipole radiation is the result of the shift between the center of charge and center of mass, around which the nucleus rotates. This polarization effect is due to the octupole deformation which is discussed by Bohr and Mottleson [26] and Strutinsky [27] within the liquid drop model. The induced dipole moment which involves the quadrupole, octupole, and hexadecapole deformations can be evaluated from the expression

$$D_0 = C_1 A z e \beta_3 \left(\beta_2 + \frac{88}{27\sqrt{5}} \beta_4 \right) , \qquad (13)$$

where C_1 is a function of symmetry energy coefficient C and is sensitive to the model assumptions. Leander *et al.* [17] performed the calculations of D_0 as a function of β_3 for ^{144}Ba and ^{148}Sm. The ^{149}Sm nucleus has one

TABLE V. Dipole moment calculation of ^{149}Sm and ^{151}Sm.

Nucleus	I_i	$I_f(E1)$	$I_f(E2)$	$B(E1)/B(E2)$ $(10^{-6}$ fm$^{-2})$	$Q_0(e\,\text{fm}^2)^{\text{a}}$	$D_0(e\,\text{fm})^{\text{a}}$
^{149}Sm	$\frac{15}{2}^+$	$\frac{13}{2}^-$	$\frac{11}{2}^+$	2.12 ± 0.04	-53.27 ± 13.85	0.08 ± 0.02
	$\frac{19}{2}^+$	$\frac{17}{2}^-$	$\frac{15}{2}^+$	27.91 ± 0.31	-34.47 ± 8.96	0.09 ± 0.02
	$\frac{31}{2}^+$	$\frac{29}{2}^-$	$\frac{27}{2}^+$	266.63 ± 8.00	-23.37 ± 6.08	0.20 ± 0.05
	$\frac{17}{2}^-$	$\frac{15}{2}^+$	$\frac{13}{2}^-$	109.0 ± 2.18	-40.59 ± 10.55	0.20 ± 0.05
	$\frac{21}{2}^-$	$\frac{19}{2}^+$	$\frac{17}{2}^-$	230.95 ± 5.77	-30.89 ± 8.03	0.37 ± 0.1
^{151}Sm	$\frac{21}{2}^-$	$\frac{19}{2}^+$	$\frac{17}{2}^-$	4.39 ± 0.22	-270.79 ± 27.08	0.25 ± 0.03
	$\frac{31}{2}^+$	$\frac{29}{2}^-$	$\frac{27}{2}^+$	27.15 ± 1.22	-176.80 ± 17.68	0.47 ± 0.06

$^{\text{a}}$Large error is due to the associated error in experimental q-moment values.

neutron more than the core ^{148}Sm. It is expected that both nuclei may have similar β_3 deformation supported by comparable $E1$ and $E2$ branching ratios and D_0 values. Therefore, by using the curve of D_0-β_3 for ^{148}Sm and taking the values of β_2 to be 0.13 for ^{149}Sm [3], 0.2 for ^{151}Sm [13] and $\beta_4 = 0.03$ for both the nuclei, C_1 has been estimated for all values of D_0 for ^{149}Sm. It has been found to be

$$C_1 = 2.003^{+0.087}_{-0.159} \times 10^{-3} \text{ fm} .$$

This is higher than Strutinsky's numerical estimate of $C_1 = 0.69 \times 10^{-3}$ fm $(C_1 = (9/56\sqrt{35})e^2/\pi C$ fm$)$ obtained considering the Fermi gas symmetry energy coefficient $C = 18$ MeV, which, however, neglects the surface effects.

V. SUMMARY AND CONCLUSION

The experimental study of the structure of ^{149,151}Sm nuclei has been undertaken to test the evidence of octupole deformation induced by nuclear rotation. Two pairs of alternating parity bands classified by $s = \pm i$ were observed in ^{149}Sm. In the ^{151}Sm nucleus one pair of such alternating parity band of simplex quantum number $s = -i$, connected by $E1$ transition has been found.

The properties of parity splitting were discussed. It is found that signature splitting may contribute to the values of δE along with parity splitting.

Collective rotational parameters, i.e., effective moment of inertia, aligned angular momentum, and experimental Routhians were evaluated from the measurements. Hence the values of the quasiparticle Routhians and single-particle aligned angular momentum were derived. These results show remarkable similarities with those of odd-A ^{221,223}Th nuclei, the only exception being the quenching of single-particle alignment and the development of stable octupole deformation taking place at higher rotational frequency for ^{149,151}Sm.

The intrinsic dipole moment D_0 originating from the octupole deformation has been estimated and the average values thus obtained are compared and found to be very close to the theoretical values for ^{148}Sm [17]. Using the β_3 values of ^{148}Sm corresponding to each D_0 value from the present work, the C_1 parameter, a function of symmetry energy coefficient of liquid drop model of Strutinsky, has been obtained.

The behavior of the two nuclei under study are dissimilar if we consider them in terms of quadrupole-octupole deformation. ^{149}Sm with one neutron less than $N = 88$ shows a characteristic excitation, exhibited by even-even neighboring nuclei. The parity doublet states are better developed in ^{149}Sm than in ^{151}Sm. The observation of stronger $E2$ and $M1$ transitions than $E1$ in ^{151}Sm supports the higher quadrupole deformation. However, the absence of strong $E1$ transitions does not exclude the possibility of octupole deformation in this nucleus [9,28].

Most of the theoretical studies have been aimed at for the actinides where the experimental data are rich. A recent work [29] has dealt considerably with the shape changes in the lanthanides using the cranking model with average Woods-Saxon potential and pairing. Detailed theoretical studies are necessary for the better understanding of the phenomenon of reflection asymmetry in the lanthanides.

[1] A. Wolf, R. F. Casten, Phys. Rev. C **36**, 851 (1987).

[2] J. Suhonen, Phys. Lett. B **193**, 405 (1987).

[3] E. Hammarén, E. Liukkonen, M. Piiparinen, J. Kownacki, Z. Sujkowski, Th. Lindblad, and H. Ryde, Nucl. Phys. **A321**, 71 (1979).

[4] G. Vandenput, P. H. M. Van Assche, L. Jacobs, J. M. Van den Cruyce, R. K. Smither, K. Schreckenbach, T. von Egidy, D. Breitig, H. A. Baader, and H. R. Koch, Phys. Rev. C **33**, 1141 (1986).

[5] W. Urban, R. M. Lieder, W. Gast, G. Hebbinghaus, A. Krämer-Flecken, K. P. Blume, and H. Hübel, Phys. Lett. B **185**, 331 (1987).

[6] W. Urban, R. M. Lieder, W. Gast, G. Hebbinghaus, A. Krämer-Flecken, T. Morek, T. Rzaça-Urban, W. Nazarewicz, and S. L. Tabor, Phys. Lett. B **200**, 424 (1988).

[7] W. Urban, J. C. Bacelar, W. Gast, G. Hebbinghaus, A. Krämer-Flecken, R. M. Lieder, T. Morek, and T. Rzaça-Urban, Phys. Lett. B **247**, 238 (1990).

[8] W. J. Vermeer, M. K. Khan, A. S. Mowbray, J. B. Fitzerald, J. A. Cizewski, B. J. Varley, J. L. Durell, and W. K. Phillips, Phys. Rev. C **42**, R1183 (1990).

[9] P. D. Cottle, T. Glasmacher, and K. W. Kemper, Phys. Rev. C **45**, 2733 (1990).

[10] R. K. Sheline, A. K. Jain, and K. Jain, Phys. Rev. C **38**, 2952 (1988).

[11] P. Šimecek, R. Julin, S. Juutinen, M. Kortelahti, S. Kumpulainen, D. Nosek, A. Pakkanen, and I. Procházka, Z. Phys. A **333**, 323 (1989).

[12] P. Kleinheinz, A. M. Stefanini, M. R. Maier, R. K. Sheline, R. M. Diamond, and F. S. Stephens, Nucl. Phys. **A283**, 189 (1977).

[13] W. B. Cook, M. W. Johns, G. Lovhoiden, and J. C. Waddington, Nucl. Phys. **A259**, 461 (1976).

[14] W. Gelletly, R. Chapman, G. D. Dracoulis, S. Flanagan, A. J. Hartley, J. N. Mo, W. Scheck, R. M. Lieder, H. Beuscher, W. F. Davidson, A. Neskakis, and H. M. Jager, J. Phys. G **2**, L1 (1976).

[15] J. M. Chatterjee, Somapriya Basu, R. K. Chattopadhyay, K. Kar, D. Banik, R. P. Sharma, and S. K. Pardhasaradhi, Z. Phys. A **344**, 149 (1992).

[16] J. A. Szücs, M. W. Johns, and B. Singh, Nucl. Data Sheets **46**, 1 (1986).

[17] G. A. Leander, W. Nazarewicz, G. F. Bertsch, and J. Dudek, Nucl. Phys. **A453**, 58 (1986).

[18] A. K. Jain, R. K. Sheline, P. C. Sood, and Kiran Jain, Rev. Mod. Phys. **62**, 393 (1990).

[19] M. Dahlinger, E. Kankeleit, D. Habs, D. Schwalm, B. Schwartz, R. S. Simon, J. D. Burrows, and P. A. Butler, Nucl. Phys. **A484**, 337 (1988).

[20] W. Nazarewicz and P. Olanders, Nucl. Phys. **A441**, 420 (1985).

[21] P. Bonche, P. H. Heenen, H. Flocard, and D. Vautherin, Phys. Lett. B **175**, 387 (1986).

[22] B. Singh, J. A. Szücs, and M. W. Johns, Nucl. Data Sheets **55**, 185 (1988).

[23] P. Barreau, L. Roussel, and R. J. Powers, Nucl. Phys. **A364**, 446 (1981).

[24] K. Dorschel, H. Huhnermann, E. Knobl, Th. Meier, and H. Wagner, Z. Phys. A **302**, 359 (1981).

[25] K. N. Mukhin, *Experimental Nuclear Physics*, Vol. I, of *Physics of Atomic Nucleus* (Mir Publishers, Moscow, 1987).

[26] A. Bohr and B. R. Mottleson, Nucl. Phys. **4**, 529 (1957).

[27] V. M. Strutinsky, J. Nucl. Energy **4**, 523 (1957).

[28] H. Mach, W. Nazarewicz, D. Kusnezov, M. Moszynski, B. Fogelberg, M. Hellstrom, L. Spanier, R. L. Gill, R. F. Casten, and A. Wolf, Phys. Rev. C **41**, R2469 (1990).

[29] W. Nazarewicz and S. L. Tabor, Phys. Rev. C **45**, 2226 (1992).

[30] L. K. Peker, Nucl. Data Sheets **59**, 393 (1990).